

Flutter suppression of long-span suspension bridge with truss girder

Kai Wang^{1,2a}, Haili Liao^{*1} and Mingshui Li^{1b}

¹Research Centre for Wind Engineering, Southwest Jiaotong University, Chengdu, Sichuan 610031, China

²Sichuan Railway Investment Group Company Limited, Chengdu, Sichuan 610041, China

(Received January 22, 2016, Revised July 22, 2016, Accepted July 27, 2016)

Abstract. Section model wind tunnel test is currently the main technique to investigate the flutter performance of long-span bridges. Further study about applying the wind tunnel test results to the aerodynamic optimization is still needed. Systematical parameters and test principle of the bridge section model are determined by using three long-span steel truss suspension bridges. The flutter critical wind at different attack angles is obtained through section model flutter test. Under the most unfavorable working condition, tests to investigate the effects that upper central stabilized plate, lower central stabilized plate and horizontal stabilized plate have on the flutter performance of the main beam were conducted. According to the test results, the optimal aerodynamic measure was chosen to meet the requirements of the bridge wind resistance in consideration of safety, economy and aesthetics. At last the credibility of the results is confirmed by full bridge aerodynamic elastic model test. That the flutter reduced wind speed of long-span steel truss suspension bridges stays approximately between 4 to 5 is concluded as a reference for the investigation of the flutter performance of future similar steel truss girder suspension bridges.

Keywords: steel truss; suspension bridge; section model; aerodynamic measure; wind tunnel testing

1. Introduction

There are two main types of main beams in suspension bridges: steel box and steel truss beams. Despite that steel box beam has many advantages such as low consumption of steel, constructing convenience, light weight and beauty, steel truss beam is still recommended as the first choice in the construction of double-deck highway bridges, highway-railway dual-purpose bridges, bridges mainly transporting long large objects and those suspension bridges built in mountainous areas where bridge erection is difficult. With good ventilation and large vertical stiffness, suspension bridges have many advantages in long span bridges construction period. At present, numerous long-span suspension bridges with steel truss beam have been built abroad, such as Akashi Kaikyo Bridge (1998) with a main span of 1991 m in Japan and Golden Gate Bridge (1937) in USA with a main span of 1280 m. With the economic development in China, transportation infrastructure construction has become the most important issue in development of the western region with high

*Corresponding author, Professor, E-mail: hlliao@home.swjtu.edu.cn

^a Ph.D., Email: wangk1010@126.com

^b Professor, Email: lms_rcwe@126.com

mountains, lofty hills and complex terrains. For completed bridges in these regions with mountainous terrains and deep valleys, long-span suspension bridges with steel truss beam are adopted in Xiangxi Aizhai Bridge (2012) in Hunan Province with a main span of 1176 m and Baling River Bridge (2009) in Guizhou Province with a main span of 1088 m.

Modern bridges tend to be longer, slender and more flexible, which leads to the increase of sensitivity to the wind. The wind load has become a major load or load control in long-span bridge design. At the same time, flutter may cause damage the whole long-span bridges so that flutter is an important factor in the design of bridges. Therefore, analysis of bridges' aerodynamic stability reveals its great significance. Because the numerical method may not solve aerodynamic stability, currently wind tunnel test is the main technique to investigate flutter stability of the main beam.

With a flexible structure and small damp along with a low vibration frequency, the long span suspension bridge is sensitive to the wind. So the wind resistance safety has become a significant factor in the design of long span suspension bridges. Since the Tacoma Bridge (1940) in USA was destructed by wind, the investigation of flutter stability of the suspension bridges has gained wide attention.

After the wind destruction accident of the Old Tacoma Bridge, in order to explore the wind destruction mechanism, the investigation committee of the accident conducted a scale model wind tunnel test. Von Karman, Fr.Bleich etc, famous aerodynamicists, adopted the classical aerodynamic theory to analyze the reason of the accident. Fr.Bleich testified that it was the flutter that had caused wind destruction of the bridge; and he came up with the method of 2-D dynamic analysis to calculate the flutter critical wind speed. The new Tacoma Narrows Bridge was redesigned and constructed in the original site according to the former span. In order to improve the wind-resistance performance of the main beam of the new bridge, the stiffening girder was replaced by the steel truss girder. In addition, comparative research of the wind-resistance performance of the main beam was done by conducting the wind tunnel test, which was greatly improved by opening several zonal porosities on the surface of the bridge. The wind tunnel test was a big success in the design of the new Tacoma Bridge, which becomes an indispensable means of the long-span suspension bridge designs.

Bleich (1948) adopted the plate self-excited aerodynamic force theory to investigate the flutter of suspension bridges for the first time. Scalan (1971) has devoted himself in the flutter stability study of the bridges and has formulated a method to combine the theoretical analysis with the wind tunnel tests. Ito *et al.* (1985) used the probabilistic analysis method to study the flutter reliability of the Akashi-Kaikyo Bridge. The flutter stability of the Akashi-Kaikyo Bridge was improved by using the solution of lower central stabilized plate and permeability openings on the bridge. Yang, Ge *et al.* (2007) have studied the change of the aerodynamic shape and the width of permeability openings of the box girder of the Xihoumen Bridge. Chen, Ouyang *et al.* (2009) have conducted research on the impacts that the central stabilized plates had on the flutter stability of the steel truss bridges. They claimed that the principle of the central stabilized plates was to transfer the flutter shape from single degree-of- freedom to bending-torsional coupling in order to improve the flutter critical wind. Liu *et al.* (2005) have used the active-control wing plate to suppress the flutter of the suspension bridge through analysis and calculation.

In this paper, the flutter suppression effects of different flutter control measures on a few large span steel truss girder suspension bridges with several different sections in mountainous areas will firstly be investigated. Those measures include bridge deck with central slot, upper central stabilized plate, lower central stabilized plate and horizontal stabilized plate. Then the law of flutter suppression measures of steel truss girder suspension bridges with different cross sections

are summarized.

2. Engineering background

As for flutter phenomenon in bridges, active and passive control methods are the two main approaches to. As active control method is not mature both in theory and in practice, currently passive control method is mainly adopted in bridges, such as bridge deck with central slot, upper central stabilized plate, lower central stabilized plate and horizontal stabilized plate. In this paper, three long-span suspension bridges with steel truss beam built in mountainous areas are used as examples to study flutter control methods.

Qingshui River Bridge (Guizhou Province, China), Dimu River Bridge (Guizhou Province, China), and Qingjiang River Bridge (Hubei Province, China) are all built across grand canyons with steep terrains that change rapidly on both sides and a depth of hundreds of meters. All the three bridge are located in typical mountain valley wind fields. Qingshui River Bridge is a steel truss suspension bridge with a main span of 1130 m, which is a plate-truss composite system, the girder is 27.0 m in width, 7.0 m in depth (shown in Fig. 1). Dimu River Bridge is a steel truss suspension bridge with a main span of 538m, which is a plate-truss separation system. The main beam is composed of a 27 meter-wide and 4.5 meter-high steel truss beam and a 0.8 meter-high orthotropic plate which is placed on the steel truss beam (shown in Fig. 2). Qingjiang River Bridge is a steel truss suspension bridge with a main span of 420 m, which is a plate-truss separation system. The main beam is composed of a 13.3 meter-wide and 3.6 meter-high steel truss beam and a 0.8 meter-high concrete plate on the steel truss beam (shown in Fig. 3).

A recurrence period of 100 years was chosen by the designer in wind resistant design of the bridge. The yearly maximum mean winds averaged within 10 minutes. The size and the design wind speeds of the three bridges are shown in Table 1.

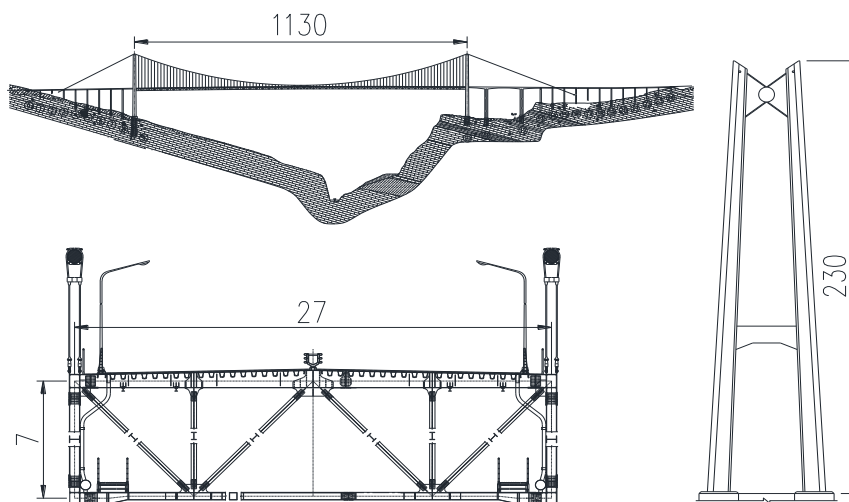


Fig. 1 General view of Qingshui River Bridge

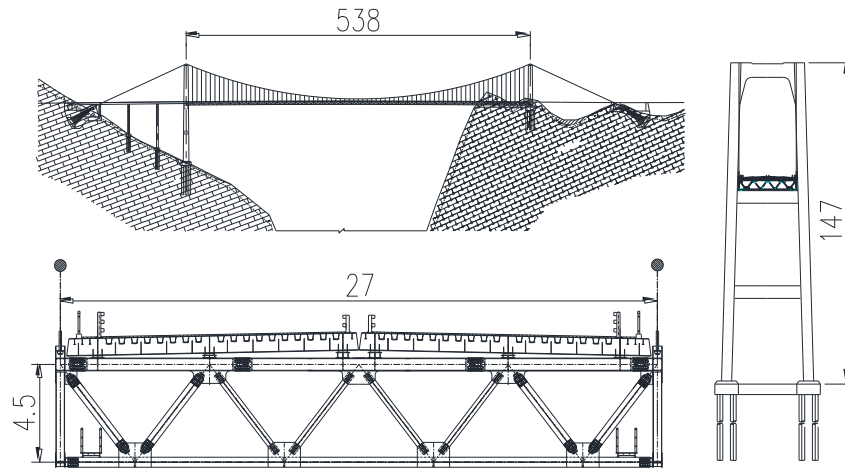


Fig. 2 General view of Dimu River Bridge

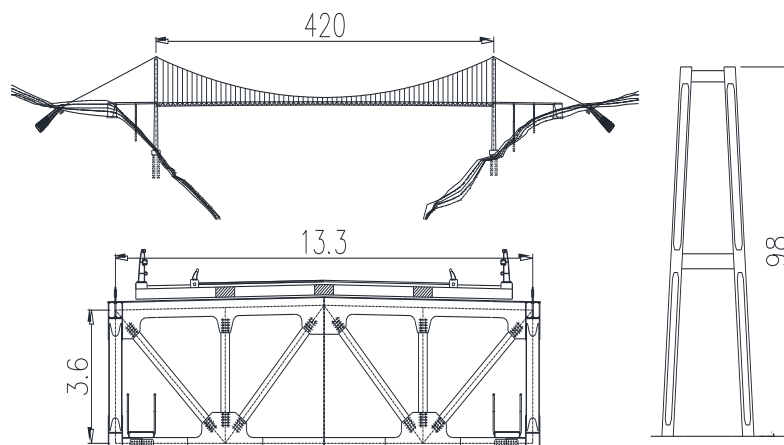


Fig. 3 General view of Qingjiang River Bridge

Table 1 The size and the design wind speeds of the three bridges

Bridge name	Long of main span (m)	Width of girder (m)	Depth of girder (m)	Design wind speed (m/s)	Flutter check wind speed(m/s)
Qingshui River Bridge	1130	27	7	29.4	46.6
Dimu River Bridge	538	27	5.3	34.8	57.6
Qingjiang River Bridge	420	13.3	4.4	31.0	52.1

3. Experimental technique

Flutter is a dangerous self-excited divergent vibration. When the wind speed reaches a bridge's flutter critical wind speed, the vibrating bridge can constantly absorb energy from the wind through the feedback of the airflow, which will gradually increase the amplitude of vibration until the structural collapse. In bridge wind resistance design, flutter critical wind speed must be higher than the equivalent flutter check wind speed.

Flutter critical wind speed of main beam at different attack angles is tested through aerodynamic section model wind test. The suppression of wind-induced vibration of the model is preliminarily evaluated. If the divergent flutter instability of the bridge occurs when wind speed is lower than flutter check wind speed, aerodynamic optimization measures must be taken.

Specialized device in wind tunnel test is used in testing aerodynamic model of bridge. The model is suspended on the support by eight springs. Two dimension vibration systems can rotate and also can move vertically. The support is located outside the wind tunnel so that wind field can't be disturbed by it. Schematic diagram of model test is shown in Fig. 4.

The wind tunnel (Type: XNJD-1) of Southwest Jiaotong University, a closed circuit wind tunnel with two tandem closed test sections, was used to carry out the investigation. The dimension of the test section is 2.4 m×2.0 m×16.0 m ($W \times H \times L$), with wind speed adjustable from 1 m/s to 45.0 m/s (turbulent intensity < 0.5%). A test set-up, which was specially designed to carry out wind-induced vibration testing of bridge girder section and mounted on the outside walls of wind tunnel, was used in this investigation. The model was suspended by four pairs of linear springs and it could vibrate vertically and torsionally.

3.1 Similarity rules

When direct measurement is used to conduct flutter test, the requirements of geometric shape similarity between the model and real bridge must be satisfied, i.e., the following three dimensionless parameters consistency condition should also be satisfied

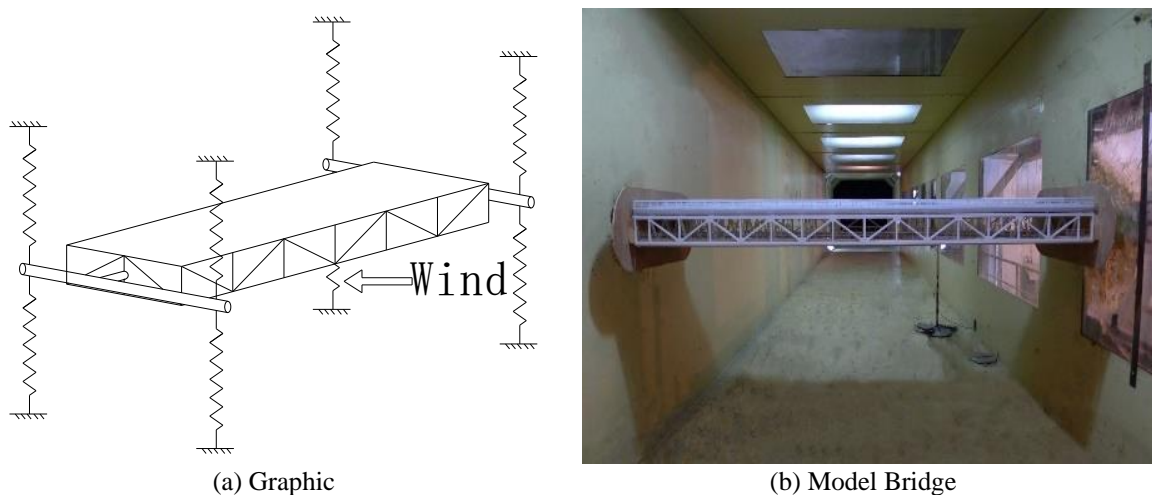


Fig. 4 Schematic diagram of model test

$$\begin{aligned} \text{Elastic Parameter: } & \frac{U}{\omega_h B}, \frac{U}{\omega_\alpha B} \text{ or } \frac{\omega_\alpha}{\omega_h} \\ \text{Inertial Parameter: } & \frac{m}{\rho b^2}, \frac{I_m}{\rho b^4} \text{ or } \frac{r}{b} \\ \text{Damping Parameter: } & \xi_h, \xi_\alpha \end{aligned}$$

where U is the average wind speed; B is the width of deck, ω_h and ω_α are the bending and torsional vibration natural frequencies, respectively; m and I_m are mass and mass moment of inertia per unit length of the bridge, respectively; ρ is air density; r is the radius of inertia, $r = \sqrt{I_m/m}$; b is half of the width of the bridge, $b = B/2$; ξ_h and ξ_α are vertical bending and torsion vibration damping ratios, respectively.

3.2 The model

In order to control the model's mass and mass moment of inertia and ensure that the model itself has enough rigidity, high-quality wood and plastic are used to make the model, which has a certain geometric scale. Upper and lower chord and plates at both ends of the beam are made of wood. Other truss, deck, railings, maintaining roadway of the beam are made of engineering plastics that are made by the CNC engraving machine. To ensure the aerodynamic characteristics of 2D flow around main beam section, plates are installed at both ends of the main beam. Anemometer is fixed in front of the model where wind filed will not be disturbed to monitor the wind speed in the wind tunnel.

3D wind-induced vibration of the beam is simplified to bending-torsional coupling vibration in dynamic section model test. In terms of overall movement of whole bridge and bending-torsional coupling vibration in different directions, full bridge in interaction of equivalent mass and the equivalent mass moment of inertia are adopted in the test to make the system more precise.

So far, there hasn't been a widely accepted method to estimate the damping ratio of bridge structure. In China, damping ratios are recommended in Wind-resistant Design Specification for Highway Bridges as follows: 0.5% for steel bridges, 1% for composite beam bridges, 2% for concrete bridges. These values are related to main beam, the value of damping ratio of truss beam can be recommended as 0.5%. In order to obtain the safety test results, the damping ratios of vertical and torsion of the model are controlled under 0.5%.

3.3 Test method

Considering the sensitivity of the flutter critical wind speed to wind attack angle, the tests were conducted in the uniform flow field under three angles of attack (α): 0° , $+3^\circ$ and -3° . When the wind directly flows towards the bottom surface of the main beam, the wind attack angle is positive. Tests are carried out in uniform flow. For each working condition, the wind speed starts from 0 m/s with an increment of 0.2 m/s. When the wind speed is greater than 1.2 times of the flutter check wind speed, the flutter stability of the bridge meet the requirements.

Two laser displacement sensors are placed under the model in the test. These sensors can measure the displacement of the model and at the same time monitor the flutter critical wind speed

when the flutter occurs. Then wind speed ratio, which is the ratio of wind speed of model test to natural wind speed of real bridge, is used to calculate flutter critical wind speed of the real bridge. Flutter critical wind speed means critical point of transferring wind-induced vibration stable state to instable state. Dynamic test parameters of the model can be seen in Table 2.

4. Test results and discussion

The flutter critical wind speed of the three bridges can be seen in Table 3. As shown in the table, for Qingshui River Bridge, in the 0° and $+3^\circ$ wind attack angle the flutter critical wind speed is smaller than the flutter test wind speed. For Dimu River Bridge, in the $+3^\circ$ wind attack angle, the flutter critical wind speed is smaller than the flutter test wind speed. And for Qingjiang River Bridge, in the 0° and -3° wind attack angle, the flutter critical wind speed is smaller than the flutter test wind speed. All the three bridges do not meet the design requirements. Therefore aerodynamic optimization tests for the main beam are needed.

According to the results of Table 3, the flutter reduced-wind speeds of the three bridges are calculated. The flutter reduced wind speed of the world's longest span bridge—Akashi-Kaikyo Bridge (Japan) with a span of 1991 meters and Aizhai Bridge (China) with a span of 1176 meters are also calculated. Table 4 shows the flutter reduced wind speed of these five bridges.

Table 2 Main test parameters of scale section model

Bridge Name	Characteristics of Vibration	Model Scale Ratio	Frequency		Equivalent Mass/Mass Moment of Inertia	
			(Hz)		(t/m)/(kg/m.m ²)	
			Real Bridge	Model Bridge	Real Bridge	Model Bridge
Qingshui River Bridge	V-A-1	1:48	0.1660	3.37	35.70	11.1284
	V-S-1		0.1777		25.64	
	T-S-1		0.3113	5.75	3335.9	0.6284
	T-A-1		0.3887		3036.3	
Dimu River Bridge	V-A-1	1:50	0.1880	2.63	34.85	10.0280
	V-S-1		0.2290		25.07	
	T-S-1		0.4770	5.6	2427.4	0.3884
	T-A-1		0.5260		2511.3	
Qingjiang River Bridge	V-A-1	1:30	0.2103	3.25	20.99	19.2444
	V-S-1		0.2751		17.32	
	T-S-1		0.6584	7.5	394.44	0.4870
	T-A-1		0.8452		345.08	

Annotation: V—vertical, T—twist, S—symmetry, A—antisymmetric. For example: V-S-1 means the first symmetric vertical

Table 3 Flutter Critical Wind Speed of the Three Bridges

Original beam section of Qingshui River Bridge				Original beam section of Dimu River Bridge				Original beam section of Qingjiang River Bridge			
Attack angle	Critical wind speed/(m·s ⁻¹)	Check wind speed/(m·s ⁻¹)	Safety evaluation	Attack angle	Critical wind speed/(m·s ⁻¹)	Check wind speed/(m·s ⁻¹)	Safety evaluation	Attack angle	Critical wind speed/(m·s ⁻¹)	Check wind speed/(m·s ⁻¹)	Safety evaluation
-3°	>65		safety	-3°	>64		safe	-3°	44.69		unsafety
0°	46.56	46.6	unsafety	0°	>64	57.6	safe	0°	49.11	52.08	safety
+3°	36.06		unsafety	+3°	53		unsafety	+3°	>60		safety

Table 4 Flutter Reduced Wind Speed of the Bridges

Bridge name	Span/m	Critical wind U/(m·s ⁻¹)	Twist fundamental frequency f/Hz	Width of the bridge B/ m	Reduced wind speed U/fB
Akashi Kaikyo bridge	1991	29.0	0.1494	35.5	5.4679
Aizhai bridge	1176	32.9	0.2903	27.0	4.1974
Qingshui river bridge	1130	36.1	0.3113	27.0	4.2831
Dimu river bridge	538	53.0	0.4770	28.0	3.9683
Qingjiang river bridge	420	44.7	0.6584	13.3	5.1047

As seen from Table 4, the flutter reduced wind speed of long span steel truss suspension bridge stays approximately between 4 to 5. Because Qingjiang Bridge is relevantly narrower, the flutter reduced wind speed is slightly higher. With a longer span, a lower twist fundamental frequency of the main beam and a wider main beam section, the flutter reduced speed wind of the Akashi-Kaikyo Bridge is higher. Based on this rule, the flutter critical wind speed of long span steel truss suspension bridge can be calculated and evaluated.

5. Aerodynamic optimization of main girder

According to the results of section model tests, when the main beams of Qingshui River Bridge, Dimu River Bridge and Qingjiang Bridge are within the range of attack angles, the flutter critical wind speed is smaller than the flutter check wind speed. In order to make the flutter characteristic of the bridges meet the design requirements and avoid bridge collapse by wind-induced flutter, a series of wind tunnel experiments of the aerodynamic shapes of the three bridges should be carried out.

5.1 Qingshui River Bridge

The most unfavorable wind attack angle $+3^\circ$ is chosen to perform aerodynamic optimizing tests. Optimized test proposal and the results (the data in the table are converted related to the real bridge) of the beam section are shown in Table 5. Horizontal stabilized plate is installed horizontally on the outside of the upper chord of the main girder.

From Table 5, it is known that every measure has a certain effect on improving the flutter divergent wind speed of the main beam through a series of optimizing section tests. But the results vary from each other which can be seen as follows:

- The lower central stabilized plate makes a little difference to the main beam of Qingshui River Bridge. However, if the plate is higher, the flutter critical wind speed is smaller than critical test wind speed.

- By using a horizontal stabilized plate with the width of 1m, the flutter critical wind speed of Qingshui River Bridge is larger than flutter test wind speed which can meet the design requirements.

- Upper central stabilized plate can obviously increase the flutter critical wind speed of Qingshui River Bridge. When upper central stabilized plate is as high as railing, flutter critical wind speed is slightly smaller than flutter test wind speed. When upper central stabilized plate is higher than railing by 0.1 m or 0.15 m, the flutter stability of the main beam can meet the suppression of wind-induced vibration.

Based on the above analysis, wind resistance safety can be improved by sealing the median railing without changing the present beam section. Considering the safety and economy of the main beam, installing upper central stabilized plate which is higher than railing by 0.1 m is the optimal solution (shown in Fig. 5).

Table 5 Aerodynamic optimized test proposal

Measures to suppress vibration	programs	Flutter divergent wind speed/($\text{m}\cdot\text{s}^{-1}$)
Lower stabilized plate	Program 1: the height of it is 1.4 m	36.10
	Program 2: the height of it is 2.1 m	36.11
Horizontal stabilized plate	Program 3: the width of it is 0.75 m	42.49
	Program 4: the width of it is 1 m	46.11
	Program 5: the width of it is 1.1 m	50.13
	Program 6: the width of it is 1.25 m	42.11
Horizontal and lower stabilized plate	Program 7: the width of horizontal stabilized plate is 1.1 m and the height of lower stabilized plate is 2.1 m	53.66
upper stabilized plate	Program 8: upper stabilized plate is as high as railing	42.49
	Program 9: upper stabilized plate is higher than railing by 0.1 m	51.5
	Program 10: upper stabilized plate is higher than railing by 0.15 m	56.49
Upper and lower stabilized plate	Program 11: upper stabilized plate is as high as railing and the height of lower one is 2.1 m	42.77
Horizontal and upper stabilized plate	Program 12: the width of horizontal stabilized plate is 2.1 m and upper stabilized plate is as high as railing	56.41

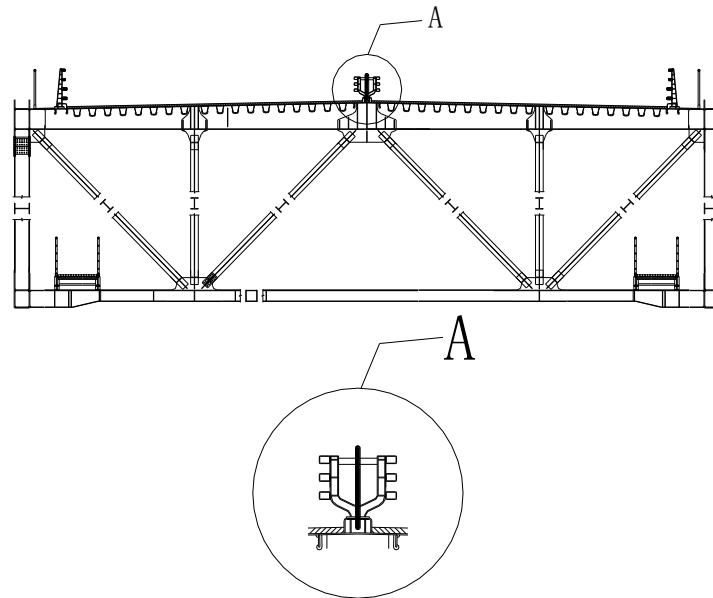


Fig. 5 Center Stabilized Plate of Qingshui River Bridge

5.2 Dimu River Bridge

For selecting the best solution, wind attack angle $+3^\circ$ which has few effects has been chosen to perform the aerodynamic optimization test. The optimization solutions and results of the main beam are listed in Table 6. The data in the table are converted to actual data of actual bridges instead of models.

As shown in Table 5, based on a series of optimization section model tests, all solutions have certain effects on increasing flutter critical wind speed, but the effects are different. The differences are as follows:

- Installing horizontal deflector, or sealing the groove, or using grille to seal the groove can only increase flutter critical wind speed by 2-3 m/s. They practically don't improve the aerodynamic performance of the main beam. And the horizontal deflector influences beauty of the bridge.

- Sealing the groove completely and installing a 0.55 or 1 meter-high central stabilized plate above the deck can increase flutter critical wind speed. The higher the central stabilized plate is, the higher the flutter critical wind speed will be. But all the flutter critical wind speed in these conditions is smaller than the flutter check wind speed. And the central stabilized plate also influences beauty of the bridge.

- Sealing the groove completely and installing a central stabilized plate with the height of 1 m, 1.5 m, 1.75 m or 2 m below the deck can increase flutter critical wind speed. When the height of the central stabilized plate is less than 1.75 m, the flutter critical wind speed increases with augment of the central stabilized plate's height. But when the height of a central stabilized plate is more than 1.75 m, the flutter critical wind speed doesn't increase any more. Therefore, once the method of sealing the groove completely and installing a central stabilized plate is adopted below

the deck to increase flutter critical wind speed, the height of the central stabilized plate should not be above 1.75 m. Under this circumstance, the flutter critical wind speed is 63 m/s. But if the central stabilized plate is too high, it will be a waste of material and increase difficulty for installation.

- Using grille to seal the groove and installing a 1 meter-high central stabilized plate above the deck at intervals. Through these solutions, when the permeability of the grille is 50%, the grille is discontinuously arranged and the upper edge of the plate is close to the surface of the main beam, the flutter critical wind speed is 64 m/s. This solution saves materials, such as grille and central stabilized plate, and reduces the wind load of the main beam. And the height of the central stabilized plate is reduced to 1 m, which is convenient for installation.

Table 6 Aerodynamic Optimization Programs

Measures to suppress vibration	Programs	Flutter Divergence Wind Speed $/(m \cdot s^{-1})$
Install horizontal deflector	Program 1: the width of horizontal deflector is 1.5 m	52
Seal the groove of main beam	Program 2	52
Seal the groove of main beam and install central stabilized plate above the deck	Program 3: the height of central stabilized plate is 0.55 m	54
	Program 4: the height of central stabilized plate is 1.10 m	57
Seal the groove of main beam and install central stabilized plate below the deck	Program 5: the height of central stabilized plate is 1.0. m	53
	Program 6: the height of central stabilized plate is 1.50 m	55
	Program 7: the height of central stabilized plate is 1.75 m	63
	Program 8: the height of central stabilized plate is 2.00 m	63
Use grille seal the groove	Program 9: permeability of the grille is 50%	53
Use grille seal the groove and install central stabilized plate below the deck	Program 10: permeability of the grille is 25% and the height of central stabilized plate is 1.00 m, which are installed all long, and the upper edge of stabilized plate close to the lower surface of the upper cross beam of the main beam.	55
	Program 11: permeability of the grille is 50% and the height of central stabilized plate is 1.00 m, which are installed all long, and the upper edge of stabilized plate close to the lower surface of the upper cross beam of the main beam.	56
	Program 12: permeability of the grille is 50% and the height of central stabilized plate is 1.00 m, which are installed at intervals, and the upper edge of stabilized plate close to the lower surface of the upper cross beam of the main beam.	58
	Program 13: permeability of the grille is 50% and the height of central stabilized plate is 1.00 m, which are installed at intervals, and the upper edge of stabilized plate close to the upper surface of the upper cross beam of the main beam.	64

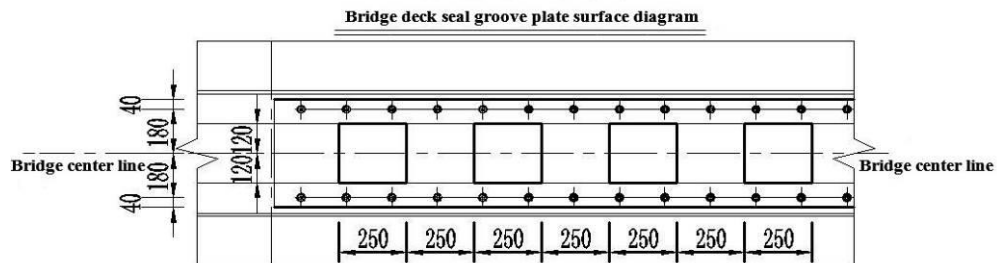


Fig. 6 Use Grille Seal the Groove of Main Beam of Dimu River Bridge

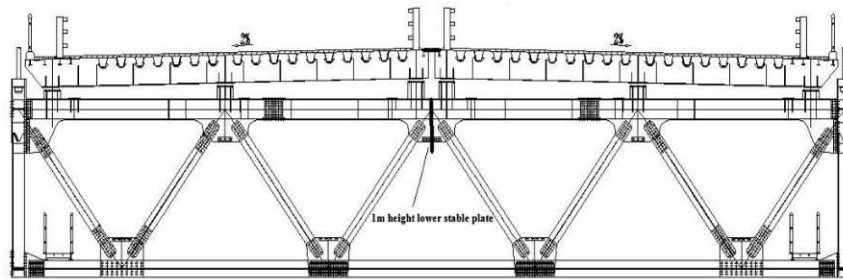


Fig. 7 Lower center Stabilized Plate of Dimu River Bridge

Based on the above analysis, the following optimization measures are recommended for Dimu River Bridge: using grille with permeability of 50% seal at the groove of the beam and installing 1 meter-high central stabilized plate at intervals, which is disconnected at the crossbeam, and making its upper edge close to the surface of the main beam (shown in Figs. 6 and 7).

5.3 Qingjiang River Bridge

For selecting the best solution, wind attack angle -3° which has few effects is chosen to perform the aerodynamic optimization test. The optimization solutions and results of the main beam are listed in Table 7. The data in the table are converted from model dimensions to that of actual bridge dimensions.

Table 7 aerodynamic optimized test proposal of Qingjiang River Bridge

Measures to suppress vibration	programs	Flutter divergent wind speed/($\text{m}\cdot\text{s}^{-1}$)
Lower stabilized plate	Program 1: the height of it is 0.6 m	45
	Program 2: the height of it is 0.75 m	49
	Program 3: the height of it is 1 m	59
	Program 4: the height of it is 1.2 m	63

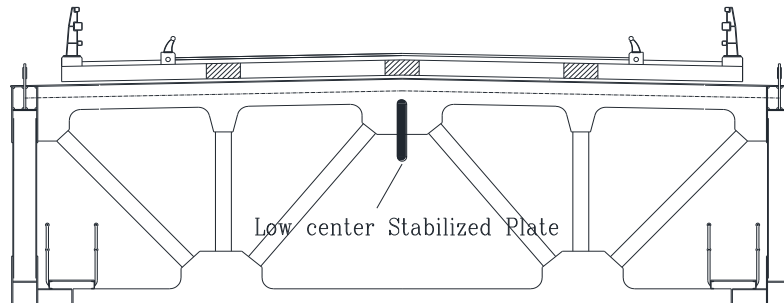


Fig. 8 Low center Stabilized Plate of Qingjiang River Bridge

Comparing results of the above several optimized test proposals, it can be concluded that installing a 1m high lower central stabilized plate in the completed stage of the bridge can notably improve the aerodynamic stability performance of the main beam of Qingjiang River Bridge and can make the flutter critical wind speed higher than the flutter check wind speed which is the most economic and effective (shown in Fig. 8).

6. Verification of flutter performance

Full bridge aerodynamic elastic model can simulate the dynamic property of the structure and reveal the interaction of the air and the structure more precisely. It is primarily used as a way to test the dynamic property of the bridge, including the static wind stability, vortex-induced vibration, flutter and galloping vibration in uniform flow. Take the full bridge aerodynamic model test of the Dimu River Bridge as an example to confirm the result of the section model flutter stability test.

The final design solution of the Dimu River Bridge was determined by the full aerodynamic elastic model test in XNJD-3 Wind Tunnel of Southwest Jiaotong University. The test section of the XNJD-3 Wind Tunnel has a length of 36 m, width of 22.5 m and height of 4.5 m. The wind speed is 1-16.5 m/s and the turbulence intensity is under 1.0% when the wind tunnel is empty. The atmospheric boundary layer can be simulated in the test section by installing spires, fence and roughness element. According to model experiment similarity theory and the topography of the bridge site, the full bridge aerodynamic elastic model was designed under the scale ratio of 1:60. Full bridge model and section girder model are shown in Figs. 9 and 10.

The full aerodynamic elastic model is used to test the flutter critical wind under the attack angle of -3° , 0° and $+3^\circ$ in uniform and turbulent flow where flutter instability did not happen when the test wind speed is lesser than the flutter check wind speed. Table 8 shows the flutter critical wind calculated by theoretical analysis and test results, respectively. From the table, flutter critical wind under different attack angles were close, which can be concluded that the bridge had a rather good dynamic stability property and the flutter critical wind speed were higher than the flutter check wind speed under different attack angle in uniform flow. In conclusion, the results of the full aerodynamic elastic model test are slightly larger than those of the section model test, which confirmed that the results of the section model test are more precise.



Fig. 8 Low center Stabilized Plate of Qingjiang River Bridge



Fig. 10 Section girder model

Table 8 Comparison of the flutter critical wind speed of test and theoretical analysis in uniform flow

Method	Attack angle		
	-3°	0°	+3°
Full bridge aerodynamic elastic model test(m/s)	>75	>75	72
Theoretical analysis(m/s)	>76	>76	73

7. Conclusions

By studying section model wind tunnel test and suppression of flutter vibration of Qingshui River Bridge, Dimu River Bridge and Qingjiang River Bridge, conclusions are drawn as follows:

- The aerodynamic performances of different truss beams are various, and their sensitivity to wind are also distinct from one another. When the wind attack angle is positive, flutter stability of Qingshui River Bridge and Dimu River Bridge are poor. However, when the wind attack angle is

negative, flutter stability of Qingjiang River Bridge is poor.

- Different solutions of aerodynamic optimization are applied to distinct truss girders, but they do not have a uniform law.
- By adopting proper aerodynamic optimization solutions, the flutter issue of all the truss girders can properly be solved.
- The height of upper central stabilized plate and lower central stabilized plate, and width of horizontal stabilized plate in the installation have great impacts on flutter divergent wind speed. Parameters such as installation position, the width and height, and whether continuous or not should be determined by wind tunnel test.
- Results of the full aerodynamic elastic model tests confirmed the reliability of the solving the flutter stability of the truss girders by section model tests.

Acknowledgements

Financial support from National Natural Science Foundation of China (Project No. 51378442), National Natural Science Foundation of China (Project No. 51478402), Science and technology project of Ministry of Transportation of China (Project No. 201231835250), and Commanding Department of the three bridges (Qingshui River Bridge at Guizhou, Dimu River Bridge at Guizhou, Qingjiang River Bridge at Hubei) are gratefully acknowledged.

References

- Agar, T.J.A. (1989), "Aerodynamic flutter analysis of suspension bridges by a modal technique", *Eng. Struct.*, **11**(2), 75-82.
- Agar, T.J.A. (1991), "Dynamic instability of suspension bridges", *Comput. Struct.*, **41**(6), 1321-1328.
- Beith, J.G. (1998), "A practical engineering method for the flutter analysis of long-span bridges", *J. Wind Eng. Ind. Aerod.*, **77-78**, 357-366.
- Bucher, C.G. and Lin, Y.K. (1988), "Effect of span wise correlation of turbulence field on the motion stochastic stability of long-span bridges", *J. Fluid. Struct.*, **2**(5), 437-451.
- Chen Z.Q., Ouyang, K.J., Niu, H.W. *et al.* (2009), "Aerodynamic mechanism of improvement of flutter stability of truss-girder suspension bridge using central stabilizer", *China Journal of Highway and Transport*, **22**(6), 53-59.
- Chen, X., Matsumoto, M. and Kareem, A. (2000), "Time domain flutter and buffeting response analysis of bridges", *J. Eng. Mech. - ASCE*, **126**(1), 7-16.
- Chen, Z.Q. and Agar, T.J. (1994), "Finite element-based flutter analysis of cable-suspended bridges (discussion)", *J. Struct. Eng. - ASCE*, **120**(3), 1044-1046.
- Davenport, A.G. (2002), "Past, present and future of wind engineering", *J. Wind Eng. Ind. Aerod.*, **90**(12-15) 1371-1380
- Dung, N.N., Miyata, T., Yamada, H. and Minh, N.N. (1998), "Flutter responses in long span bridges with wind induced displacement by the mode tracing method", *J. Wind Eng. Ind. Aerod.*, **77-78**, 367-379.
- Ge, Y.J. and Tanaka, H. (2000), "Aerodynamic flutter analysis of cable-supported bridges by multi-mode and full-mode approaches", *J. Wind Eng. Ind. Aerod.*, **86**(2-3), 123-153.
- Ge, Y.J., Xiang, H.F. and Tanaka, H. (2000), "Application of a reliability analysis model to bridge flutter under extreme winds", *J. Wind Eng. Ind. Aerod.*, **86**(2-3), 155-167.
- Ito, M. and Fujino, Y. (1985), "A probabilistic study of torsion flutter of suspension bridge under fluctuating wind", *Proceedings of the 4th International Conference on Structural Safety and Reliability*. New York.

- Katsuchi, H., Jones, N.P. and Scanlan, R.H. (1999), "Coupled flutter and buffeting analysis of the Akashi-Kaikyo Bridge", *J. Struct. Eng. - ASCE*, **125**(1), 60-70.
- Lin, Y.K. and Li, Q.C. (1993), "New stochastic theory for bridge stability in turbulent flow", *J. Eng. Mech. - ASCE*, **119**(1), 113-128.
- Miyata, T. and Yamada, H. (1990), "Coupled flutter estimate of a suspension bridge", *J. Wind. Eng. Ind. Aerod.*, **33**(1-2), 341-348.
- Namini, A., Albrecht, P. and Bosch, H. (1992), "Finite element-based flutter analysis of cable-suspended bridges", *J. Struct. Eng. - ASCE*, **118**(6), 1509-1526.
- Scanlan, R.H. (1978), "The action of flexible bridges under wind, I: flutter theory", *J. Sound Vib.*, **60**(2), 187-199.
- Scanlan, R.H. (1993), "Problematic in formulation of wind force model for bridge decks", *J. Struct. Eng. - ASCE*, **119**(7), 1433-1446.
- Scanlan, R.H. (2000), "Motion-related body-force functions in two-dimensional low-speed flow", *J. Fluid. Struct.*, **14**(1), 49-63.
- Scanlan, R.H. and Tomko, J. (1971), "Airfoil and bridge deck flutter derivatives", *J. Eng. Mech. - ASCE*, **97**(6), 1717-1237.
- Scanlan, R.H., Beliveau, J.G. and Budlong, K. (1974), "Indicial aerodynamic functions for bridge decks", *J. Sanitary Eng. - Div.*, **100**(4), 657-672.
- Tanaka, H., Yamamura, N. and Tatsumi, M. (1992), "Coupled mode flutter analysis using flutter derivatives", *J. Wind Eng. Ind. Aerod.*, **42**(1-3), 1279-1290.
- Yang, Y.X., Ge, Y.J. and Cao, F.C. (2007), "Flutter performance of central-slotted box girder section for long-span suspension bridges", *China Journal of Highway and Transport*, **20**(3), 35-40.
- Zhu, L.D., Wang, M. and Wang, D.L. (2007), "Flutter and buffeting performances of third Nanjing bridge over Yangtze river under yaw wind via aeroelastic model test", *J. Wind Eng. Ind. Aerod.*, **95**(9-11), 1579-1606.